Integrated Adjustable Phase Shifters

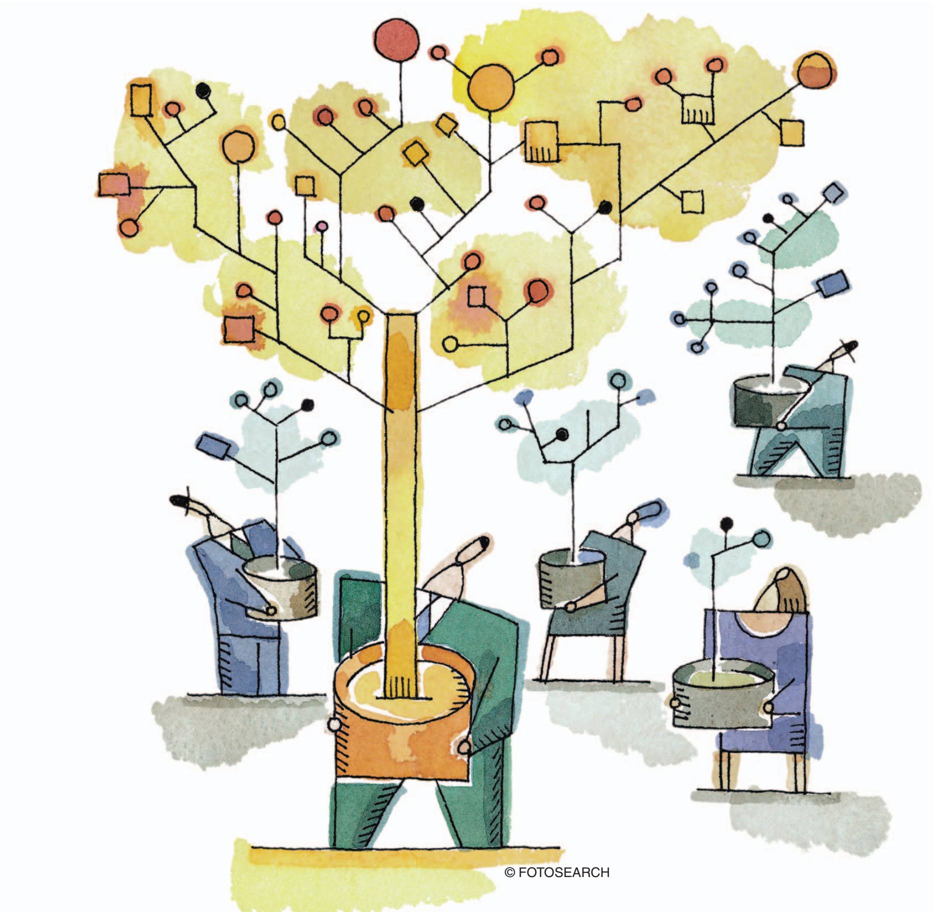
© FOTOSEARCH

Frank Ellinger, Uwe Mayer, Michael Wickert, Niko Joram, Jens Wagner, Ralf Eickhoff, Ignacio Santamaria, Christoph Scheytt, and Rolf Kraemer

When examining a monthly bank account statement, it is not only the number below the bottom line that matters. Whether that number has a minus or plus in front of it is crucial. For many technical problems, the sign matters as well. In circuits, we can change the sign by means of phase shifters. Moreover, by using phase shifters, intermediate states between the signs (including complex values) can be set in circuits. Hence, phase shifters play an important role in

Frank Ellinger (Frank.Ellinger@tu-dresden.de), Uwe Mayer, Michael Wickert, Niko Joram, Jens Wagner, and Ralf Eickhoff are with the Technical University of Dresden, Chair for Circuit Design and Network Theory, 01062 Dresden, Germany. Ignacio Santamaria is with the University of Cantabria, Department of Communications Engineering, Santander, 39005, Spain. Christoph Scheytt and Rolf Kraemer are with IHP Technologies, 15236 Frankfurt (Oder), Germany.

Digital Object Identifier 10.1109/MMM.2010.937730

The most common integrated phase shifters are based on vector modulator, distributed, reflective-type, and switched-type topologies.

electrical engineering. Unfortunately, this article does not give direct insights to change the sign of your bank statement. However, it aims to give a comprehensive overview of tunable phase shifters for radio frequency (RF) applications including cookbooklike design guidelines and performance comparisons. The focus of this article is put on phase shifters fully integrated in a chip.

Phase shifters are required for many RF systems. Examples are as follows:

- Smart antenna systems (e.g., to steer the signal beam and to optimally exploit diversity)
- Measurement equipment (e.g., for the generation and alignment of differential signals)
- Amplifier linearization systems (e.g., to cancel undesired frequency components)
- Phase-locked loops (to align the phase of the oscillator signal with that of a reference)
- Image rejection receivers (to set the phase such that the undesired image can be canceled)
- High-speed multirate front ends for optical communications (by means of multiple phase paths more sampling points are generated relaxing the clock speed at same data speed).

Requirements

For the development and optimization of integrated phase shifters, a broad range of design constraints have to be considered. Among the key design parameters and requirements are

- *Phase control range*: frequently 360° to reach the full phase space
- *Phase resolution*: theoretically each intermediate phase can be reached if the control is analogue. In this context, a linear control response is favorable to minimize the corresponding resolution required for the digital to analogue converters (DACs). The phase control resolution of switched-type phase shifters is limited by the available bit resolution
- *Group delay*: can have a significant impact on broadband signals
- *Insertion loss*: gain can be achieved by active implementations, whereas the dc power saved in passive circuits can be used for additional preamplifiers
- *Variation of insertion loss versus phase*: may require compensation e.g., by means of a variable gain amplifier (VGA)
- *Bandwidth*: the loss, phase, and group delay characteristics versus frequency are important. A high bandwidth tends to have a lower sensitivity to process and temperature variations
- *RF large signal capabilities*: for example, represented by the 1 dB compression point at the input (P_{1dB}) and the third-order intercept point at the input (IIP3)
- *Power consumption*: relevant especially for battery-driven devices and for arrays with multiple paths
- *Chip size*: as small as possible to decrease costs and device dimensions, especially for system arrays
- *Noise*: important for some applications, for example in phased array receivers, where the phase shifters are directly connected with the antennas
- *System stability*: in advance and from system perspective, the designer should carefully take into account stability at all phase states. In this context, parasitic feedback loops have to be considered, for example due to substrate coupling and the nonideal grounds on a printed circuit boards (PCBs).

This multiplicity of constraints makes the design of integrated phase shifters to a challenging task in which reasonable tradeoffs have to be found. The individual system requirements have to be considered for the optimum choice of the phase shifter topology.

Topologies

A variety of RF PCB-based [1] and fully integrated [2] active and passive phase shifter approaches have been invented to meet specific requirements. Passive approaches exhibit insertion loss while providing good large signal properties. The most common integrated phase shifters are based on vector modulator, distributed, reflective-type, and switched-type topologies. Pros and cons of the approaches, including subtypes, are summarized in Table 1. In the following sections, we will discuss the functional principles of these approaches, including cookbook-like design guidelines, IC hardware, and performance examples.

Vector Modulators

Figure 1 sketches the architecture of a vector modulator with a phase control range of 90°. The input signal is divided into two paths with 90° (I/Q) offset, which are amplitude-weighted by VGAs or attenuators, and finally combined. Various modifications are possible; for example, the phase offset may also be implemented in front of the amplifiers, the amplifiers may act as dividers or combiners, and the combiner and the phase offset may be accomplished by means of a 90° hybrid or low-pass/high-pass filters. LC (inductor capacitor) filters allow low losses but only small bandwidths, whereas resistor capacitor (RC)-based topologies enable higher bandwidth at the expense of significant loss. According to Figure 1(b), the resulting phase and magnitude are given by

$$\angle V_r = \arctan\frac{V_{90^\circ}}{V_{0^\circ}} \tag{1}$$

and

$$|V_r| = \sqrt{|V_{0^\circ}^2| + |V_{90^\circ}^2|}. \tag{2}$$

Obviously, every phase between 0° and 90° can be achieved by weighting the path gains. To obtain constant overall gain, the individual gains of the branches have to be set properly, for example, by using a look-up table.

If the amplitude control elements provide a sufficient gain control range, vector modulators can be employed for both phase and gain control.

Gain/attenuation control components with high gain control range, typically in the excess of 20 dB, are

TABLE 1. Typical qualitative performance of integrated phase shifter approaches. TL: transmission lines, LP: low-pass filter, HP: high-pass filter, g_m: transconductance, Z: impedance, L: inductance.

Type	Subtype	Comment	Phase control	Loss/ripple	BW	Size	Noise	P_{DC}
Vector modulator	VGA	Phase offsets e.g., by filters or couplers	Large	Low (gain)/low	Small/Medium	Large	Low	Medium/large
	Attenuators		Large	High/low	Medium	Medium	Similar to loss	Zero
Distributed	TL	Varactor tuned	Large	Medium/medium	Large	Very large	Similar to loss	Zero
	LP-sections	Varactor tuned	Large	Medium/medium	Large	Large	Similar to loss	Zero
		Varactor and active L tuned	Very large	Small/medium	Very large	Large	Large	Medium/large
Reflective type	Coupler based	Varactor tuned	Small	Small/small	Medium	Medium	Similar to loss	Zero
		Varactor tuned, resonated with L	Medium	Medium/large	Small	Medium	Similar to loss	Zero
		Parallel LC resonances	Large	Large/large	Small	Large	Similar to loss	Zero
		Varactor and active L tuned, resonated	Large	Medium/medium	Small	Small	Large	Medium/large
	Circulator based	Z tuning	Small	Medium/medium	Large	Small	Large	Medium
		g_m tuning	Medium	Small/small	Large	Small	Large	Medium/large
		g_m and Z tuning	Large/medium	Medium/medium	Large	Small	Large	Medium/large
Switched	TL	Simple "digital" control	Large, but resolution limited by number of bits	High/medium	Medium	Very Large	Similar to loss	Zero
	HP/LP			High/medium	Small	Large	Similar to loss	Zero

The higher the capacitance control ratio and the higher the characteristic length of the equivalent line, the higher the tuning range.

required to reach the phase range borders. Due to the high maximum gain and the high possible attenuation, cascode amplifiers are well suited. Minimum insertion phase and port impedance variations versus gain have to be guaranteed. Otherwise, phase and gain errors result, which may require calibration. In this context, optimized VGAs were presented in [3]–[6].

If the amplitude control elements provide a sufficient gain control range, vector modulators can be employed for both phase and gain control. In this case, in addition to the relative gain magnitudes, the absolute values of the gain are set. Vector modulators require no special devices such as optimized varactors. Hence, vector modulators are well suited for integration in a variety of common technologies.

Typically, to achieve 360° phase control, four paths, each exhibiting phase offsets of 90°, are required. At any given time, only two phase branches are selected by switches. Hence, the number of VGAs can be reduced to two by path switching. The four phase paths can, for example, be generated by using optimized quadrature allpass filters (QAFs) in a differential configuration [7]. In Figure 2, a circuit hardware example operating at 5.5 GHz in 0.18 μm CMOS with 1.5 V × 12 mA dc power, −7 dBm IIP3 at maximum gain, and 1 mm^2 chip area is shown [8]. In addition to the 360° phase control functionality, this vector modulator also provides gain control functionality with a control range from −20 dB to 1.5 dB. A circuit in 0.18 μm complementary metal–oxide–semiconductor (CMOS) operating at 15–20 GHz with 360° phase control, 6 ± 4 dB loss, less than 112 mW dc power, and 0.7 mm^2 chip area was published in [9]. A vector modulator at 50–56 GHz in 90-nm CMOS with 4.9 ± 0.9 dB loss, 23 mW dc power and 0.4 mm^2 chip area was reported in [10].

Furthermore, architectures with three parallel paths exhibiting 120° offset are possible. Referring to [11] and Figure 3, a circuit example operating at 5–5.5 GHz with

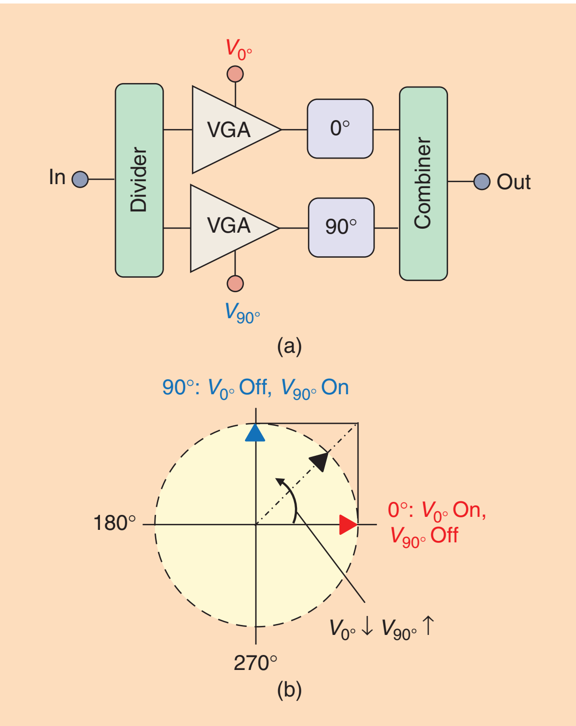

Figure 1. *Vector modulator with 90° phase control range [2], VGA: variable gain amplifier. (a) circuit architecture and (b) vector diagram.*

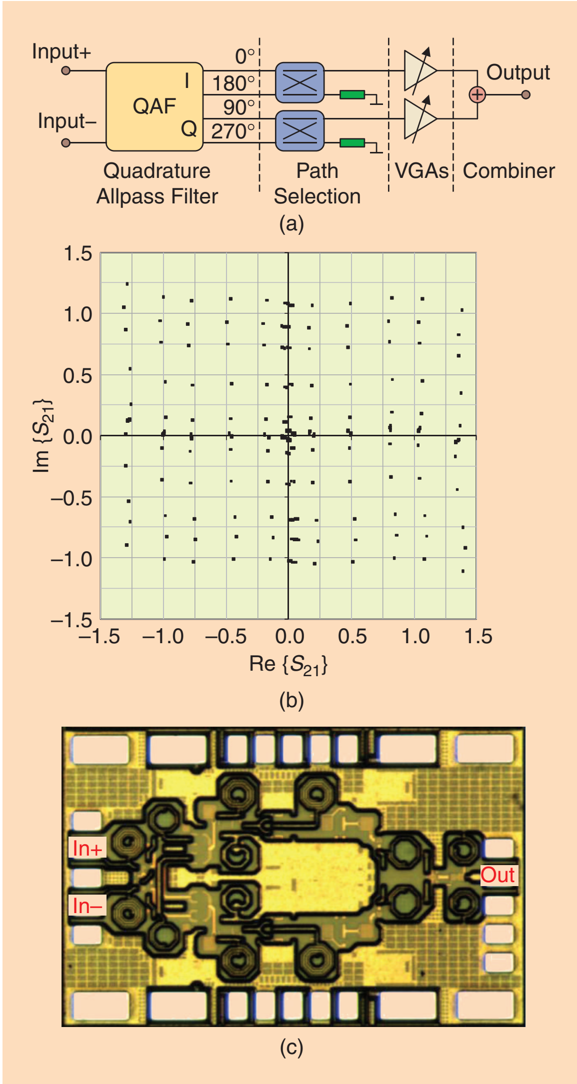

Figure 2. *Active vector modulator at 5.5 GHz implemented in 0.18 μm CMOS technology [8]. (a) Circuit architecture, (b) measured complex-plane response achieved by simple, uncalibrated variation of the control voltages, and (c) chip photo, chip size: 1.2 × 0.8 mm^2.*

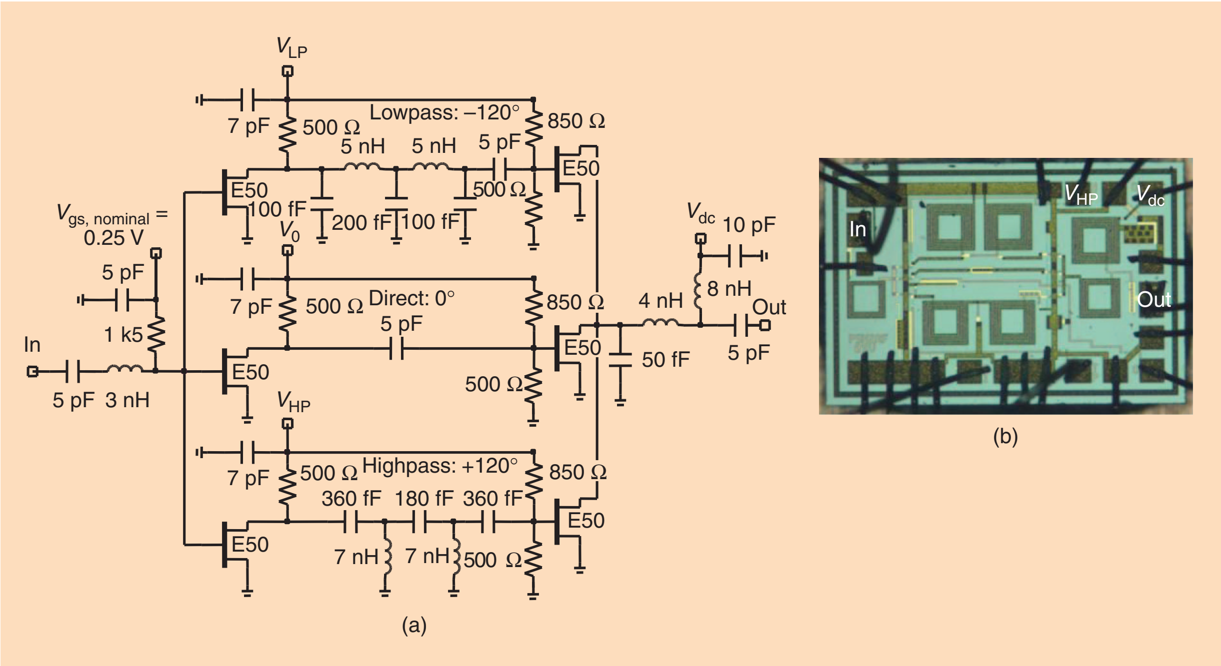

Figure 3. *Active vector modulator operating at 5–5.5 GHz in 0.6 μm GaAs technology [11]. (a) Circuit schematic and (b) chip photo, chip size: 0.9 × 1.4 mm^2.*

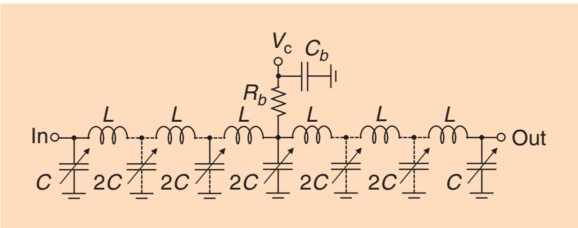

Figure 4. *Architecture of a distributed phase shifter based on low-pass filter sections [2].*

360° phase control range, 0.6 dB gain, P_{1dB} of −9 dBm, 1.5 V × 7 mA dc power and 1.3 mm^2 chip area implemented in 0.6 μm GaAs metal–semiconductor field-effect transistor (MESFET) technology was reported. A simple passive version of such a topology with zero dc power, 9 dB insertion loss, large P_{1dB} of 16.5 dBm, and 0.5 mm^2 chip area was demonstrated in [12]. By combining the control voltages of shunt and series attenuators, providing complementary attenuation the number of control voltages can be reduced to one [13].

Due to their universal applicability, moderate requirements regarding technologies (e.g., no varactors required), compact size, and ability for both phase and gain control, vector modulators are used in a variety of adaptive antenna, beamforming, and phased array systems. For details regarding such smart antenna systems using vector modulators, the reader is referred to [14]–[19].

Distributed Phase Shifters

Phase can also be controlled by tuning of varactor loaded transmission lines [20] enabling a relatively large bandwidth. To decrease circuit size, at low to

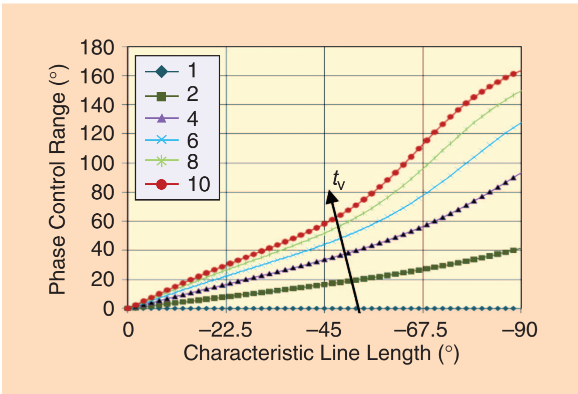

Figure 5. *Phase control range versus equivalent characteristic line length and capacitance control range t_v at a center operating frequency of one low-pass section.*

moderate frequencies, lumped-element-equivalent structures as depicted in Figure 4 are favorable. According to [21], the design equations for the inductance and the center capacitor of one Π-low-pass segment with equivalent characteristic length φ between 0° and −90° are given by

$$C = -\frac{\tan\left(\dfrac{\phi}{2}\right)}{\omega \cdot Z_0} \tag{3}$$

and

$$L = -\frac{Z_0 \sin(\phi)}{\omega}. \tag{4}$$

By varying the varactor capacitance from the minimum value C_{vmin} to the maximum value C_{vmax}, the

Phase can also be controlled by tuning of varactor loaded transmission lines enabling a relatively large bandwidth.

phase can be adjusted. As illustrated in Figure 5, the higher the capacitance control ratio

$$t_v = \frac{C_{v\max}}{C_{v\min}}, \tag{5}$$

and the higher the characteristic length of the equivalent line, the higher the tuning range. The characteristic length determines the difference in frequency between the operating frequency and the resonance frequency of the LC filters where maximum phase variations are obtained. Unfortunately, higher inductance values are required for increased characteristic line lengths typically leading to raised loss. Hence, a tradeoff between maximum phase control range and minimum insertion loss has to be chosen. As a reasonable rule of thumb, an equivalent characteristic length of 55° per section is suggested. By cascading low-pass sections, the phase control range can be multiplied.

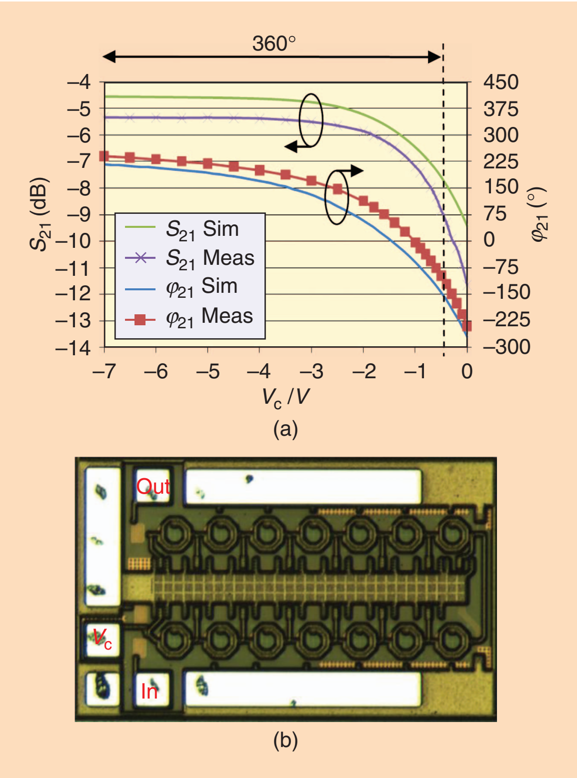

Figure 6. *Varactor-tuned equivalent-transmission-line phase shifter operating at 4–6 GHz with 360° phase control in 0.18 μm CMOS technology [22], V_c denotes the control voltage, $\varphi_{21} = \angle(S_{21})$. (a) Gain and phase versus control voltage at 5.2 GHz and (b) chip photo, chip size 1.3 × 0.8 mm^2.*

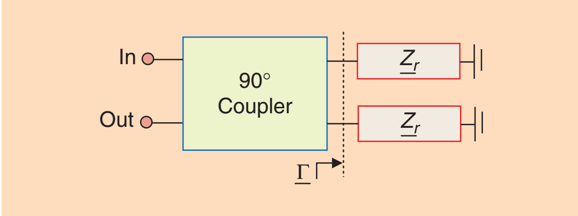

Figure 7. *Circuit topology of the reflective-type phase shifter using a branch-line coupler [2]. Phase control is obtained by varying the phase of the reflection factor Γ.*

Of course, at the same time the losses are multiplied as well. At a typical t_v of four, in ideal case, at least nine sections are required to achieve a control range of 360°. Considering the impairments in silicon, such as fixed parasitic capacitances, resistive losses, process variations and enabling a bandwidth of at least 20%, in practice, a number of around 14 sections is required.

Such a circuit yielding 360° phase control plus margin and a bandwidth of at least 4.2–6.2 GHz was implemented in 0.18 μm CMOS technology [22]. The control performance and the photo with chip area of 1 mm^2 are depicted in Figure 6. At 5.2 GHz, the insertion loss amounts to − 7.3 ± 2 dB. A modified version, optimized for low loss with six low-pass sections, provides a phase control range of 195°, an insertion loss of 3.6 ± 1.5 dB, a P_{1dB} of 12 dBm and a chip area of 0.6 mm^2 [23]. The tuning range per section can be increased by tuning the inductances together with the varactors. Active inductors as reported in [24] can be used for this task.

Referring to [25], digital control of the capacitive loading of the low-pass section can also be performed using active distributed switches. The circuit has 4-bit resolution at 11.6–12.6 GHz, −3.5 ± 0.5 dB insertion loss, 26.6 mW dc power and 1.7 mm^2 chip area. A differential version of a distributed phase shifter has been presented in [26]. To compensate for losses, distributed phase shifters can be combined with distributed amplifiers [27].

Coupler-Based Reflective-Type Phase Shifters

By varying the element values of loads, the insertion phase can be varied. However, typically such variations have a nondesired impact on the input and output impedance matching of the circuit. A coupler can be used to solve this problem. The signals are reflected at the load terminals, which are isolated, by means of the coupler, from the input and output nodes of the phase shifter. The insertion phase variation of the circuit is proportional to the reflection coefficient at the reflective loads given by

$$\underline{\Gamma} = \frac{\underline{Z}_r - Z_0}{\underline{Z}_r + Z_0}, \tag{6}$$

where $\underline{Z}_r$ is the impedance of the reflective loads, which in the ideal case is reactive, as discussed later.

The reference impedance Z_0 is assumed to be resistive e.g., 50 Ω. These types of circuits are called reflective type phase shifters. The phase control can be calculated from

$$\Delta\varphi = 2\left[\arctan\left(\frac{|\mathrm{Im}(\underline{Z}_{r\max})|}{Z_0}\right) - \arctan\left(\frac{|\mathrm{Im}(\underline{Z}_{r\min})|}{Z_0}\right)\right], \tag{7}$$

where $\underline{Z}_{r\max}$ and $\underline{Z}_{r\min}$ denote the maximum and minimum reflection impedances, respectively. Let us first discuss the principle of the reflective-type phase shifter based on a 90° branch-line coupler and two equal reflective loads. The input signal is divided into two parts. Each part is reflected at one of the reflective loads. The loss of the circuit is given by

$$|\underline{S}_{21}| = 20\log(|\underline{\Gamma}|). \tag{8}$$

Referring to (8), resistive losses in the reflective load have to be avoided to minimize the insertion loss, which equals 0 dB if all elements are lossless. Thus, reactive elements are favorable for the reflective loads.

If a varactor is used as reflective load, a phase control of up to 180° can be reached if the tuning range of the varactor goes towards infinity. By resonating the varactor with an inductor L_r around the center frequency of the phase shifter, the phase control range can be increased up to 360°. However, since the tuning range of varactors is limited, the full 360° cannot be achieved in practice. A further increase of the phase control range is feasible by employing parallel loads with different resonance frequencies associated with different values of the varactor capacitances. In Figure 8, simulated reflection coefficients are plotted for four reflective load options. In these simulations, typical values and losses for integrated implementations are considered. In this specific example, the Q factors of the inductors and varactors at 5 GHz are around 15 and 30, respectively. The closer the lines are to the reference impedance (in our case 50 Ω), the higher the insertion losses due to the fact that a smaller part of the signal is reflected and a higher part is absorbed in the reflective load. Both the insertion losses and the associated ripple can be decreased by adding a transformation network, which increases the magnitude of the minimal reflection coefficient and decreases the variations of the magnitude of the reflection coefficient.

Compared to passive couplers, a much higher bandwidth can be achieved by the active circulators if broadband amplifier design techniques are used.

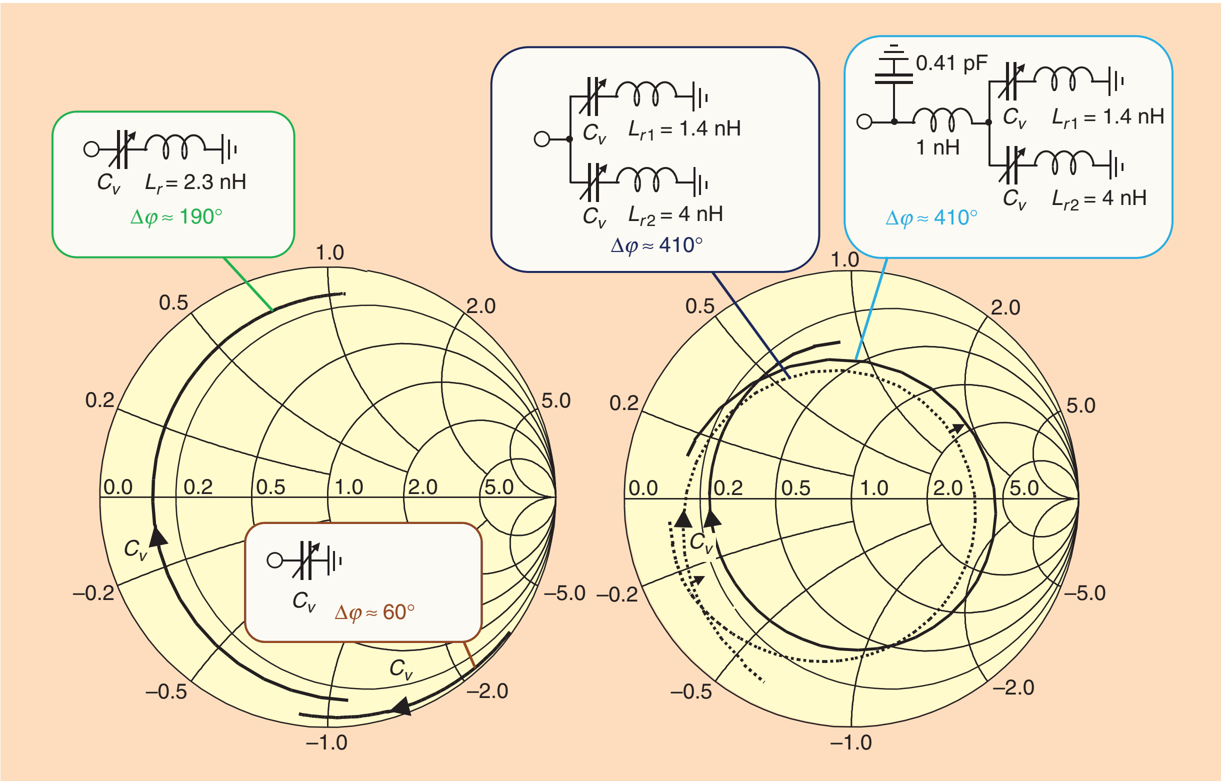

Figure 8. *Simulated reflection coefficient of reflective loads including parasitics at 5.2 GHz. The varactor capacitance is varied from 0.18 pF to 0.7 pF [28].*

The need for DACs can be circumvented by using circuits that require "digital" control voltages with only two states: high or low.

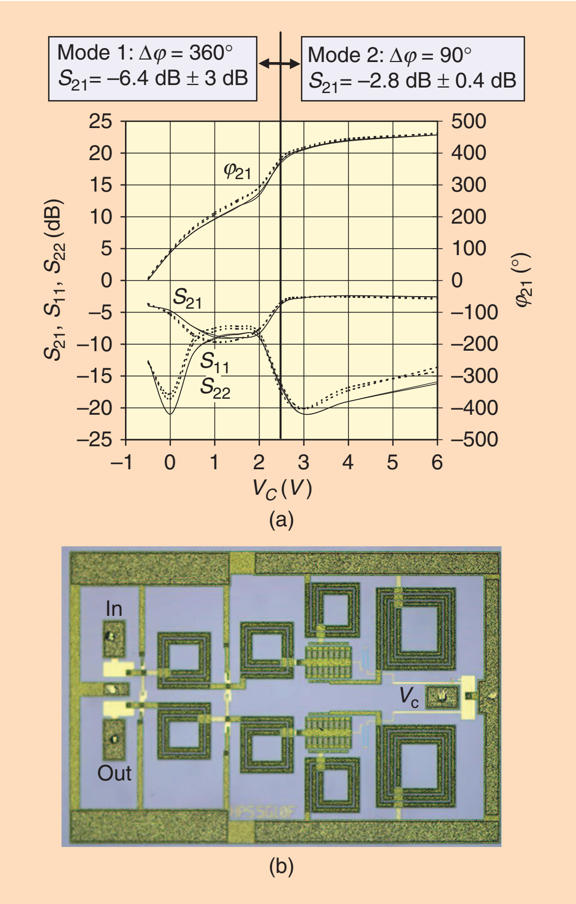

Figure 9. *Reflective-type phase shifter at 5.1–5.7 GHz with 360° phase control in 0.6 µm GaAs MESFET technology featuring a lumped-element coupler and reflective loads with two parallel resonators and transformation networks [28]. (a) Measured performance for four different samples and (b) chip photo, size: 0.85 × 1.1 mm².*

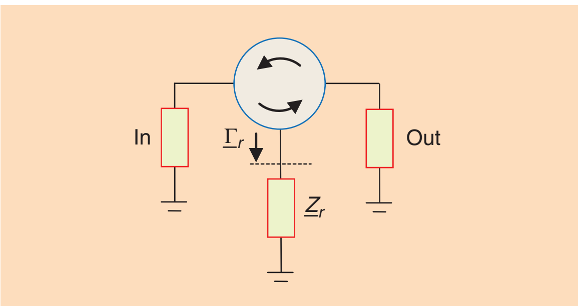

Figure 10. *Block diagram of a circulator-based phase shifter.*

A circuit operating between 5.1 and 5.7 GHz applying such reflective loads with two parallel resonators and transformation network was reported in [28]. To minimize the circuit dimensions, the coupler was realized by lumped-elements. Information regarding the design of such a lumped element coupler can be found in [29]. Figure 9 depicts the measured performance and the photo of the chip with size of 1 mm^2 realized in 0.6 µm GaAs MESFET technology. At 5.25 GHz, the circuit has a 360° phase control range, an insertion loss of 6. 4 ± 3 dB loss, and a P_{1dB} ranging from 2 to 15 dBm.

A simple implementation with reflective loads consisting of just one resonated path was demonstrated in 0.25 µm BiCMOS technology [30]. Between 14.9 and 15.7 GHz, the circuit has a phase control range of 120°, an insertion loss of 5 ± 1 dB and a chip area of 0.35 mm^2.

The phase control range can be increased by varying the varactor and the inductor of the reflective loads at the same time. This is possible by using active controllable inductors. In [31], a corresponding circuit was implemented in InP HEMT technology. Since external hyperabrupt GaAs varactors are used, the circuit is not fully integrated. The circuit yields a very low insertion loss of 0.8 dB and a phase control of more than 225° within a frequency range of 4.7–6.7 GHz, and has a power consumption of 54 mW.

Circulator-Based Reflective-Type Phase Shifters

Optionally, as shown in Figure 10, a three-port circulator is well suited to isolate the impedance changes of the reflective load on the input impedance and output impedance of the phase shifter. Based on three amplifiers, active circulators can be designed [32], [33]. Such active circulator-based reflective-type phase shifters can be optimized to have a transmission of [34]

$$\underline{S}_{21} = \frac{1 - g_{m2} \cdot \underline{Z}_r}{1 + g_{m2} \cdot \underline{Z}_r}, \tag{9}$$

where g_{m2} represents the transconductance of the amplifier driving the reflective load. Consequently, the phase can be adjusted by tuning $\underline{Z}_r$, and in addition by tuning g_{m2}. Since g_{m2} can be controlled within a wide range, relative large phase control ranges can be achieved. Moreover, high quality factor (Q) metal insulator metal capacitors with fixed values can be used for $\underline{Z}_r$, resulting in lower losses with respect to varactors exhibiting a lower Q. Compared to passive couplers, a much higher bandwidth can be achieved by the active circulators if broadband amplifier design techniques are used.

Such a circuit was reported in [34]. Implemented in 0.18 µm BiCMOS and operating from 2.5 GHz to 10 GHz, the circuit provides a phase control range of at least 90° and a gain of 0 ± 0.5 dB at 1.8 V × 4.6 mA dc power, while consuming a chip area of 0.475 mm^2 and a core circuit area as small as 0.023 mm^2. The measured phase versus control voltage and the chip photo are plotted in Figure 11.

Switched-Type Phase Shifters

Until now, the discussions have been focused on phase shifters with continuously adjustable phase by means of analog control voltages. However, typically, in practice, power consuming, costly DACs are required to generate these analog control voltages. The need for DACs can be circumvented by using circuits that require "digital" control voltages with only two states: high or low. The idea is to switch between different phase paths. The individual phases can be realized by means of delay lines, or better, because more compact, by lumped high-pass/low-pass structures. An example of a 4-bit phase shifter is illustrated in Figure 12. For design guidelines of such high-pass/low-pass sections, the reader is referred to [2]. The phase resolution of the circuit is determined by the least significant bit, which in the example shown is 22.5° corresponding to 360°/bit-amount^2. Eight (two times bit amount) digital control voltages and maybe also contact pads are required for this task. The number of control lines and contact pads can be reduced by applying a serializer circuit. Generally, the required lines or inductors are large. Thus, especially at low-to-moderate frequencies, these kinds of phase shifters require a large circuit size, thereby increasing the costs as well. The overall insertion loss and chip size increase with bit resolution. As a first-order estimation, we may estimate an insertion loss per bit between 0.5 and 2 dB.

In [35], a 5-bit switched phase shifter covering a frequency range of 17–21 GHz with 5 ± 0.6 dB insertion loss fabricated in 0.25-μm PHEMT technology was reported. An insertion loss of 14.5 ± 0.5 dB was measured for a 5-bit circuit in 0.18 μm CMOS at 12 GHz [36]. A four-element phased array system in SiGe BiCMOS at 34–39 GHz using switched-type phase shifters with 5-bit control was reported in [37].

One important design parameter for phase shifters is the phase control range.

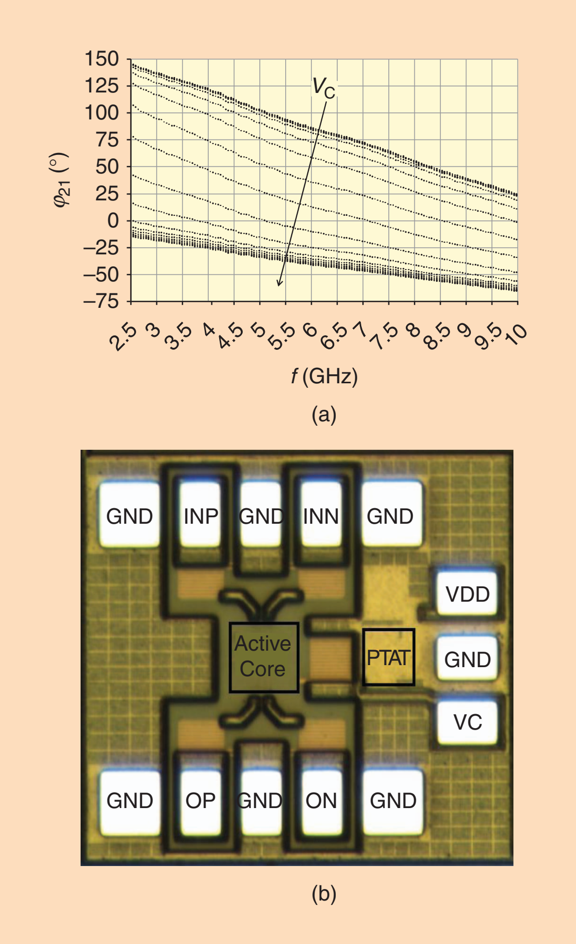

Figure 11. *Circulator-based phase shifter in 0.18 μm BiCMOS [34]; (a) measured phase versus frequency and control voltage and (b) chip photo with 0.73 × 0.65 mm^2 chip area and 0.023 mm^2 core circuit area.*

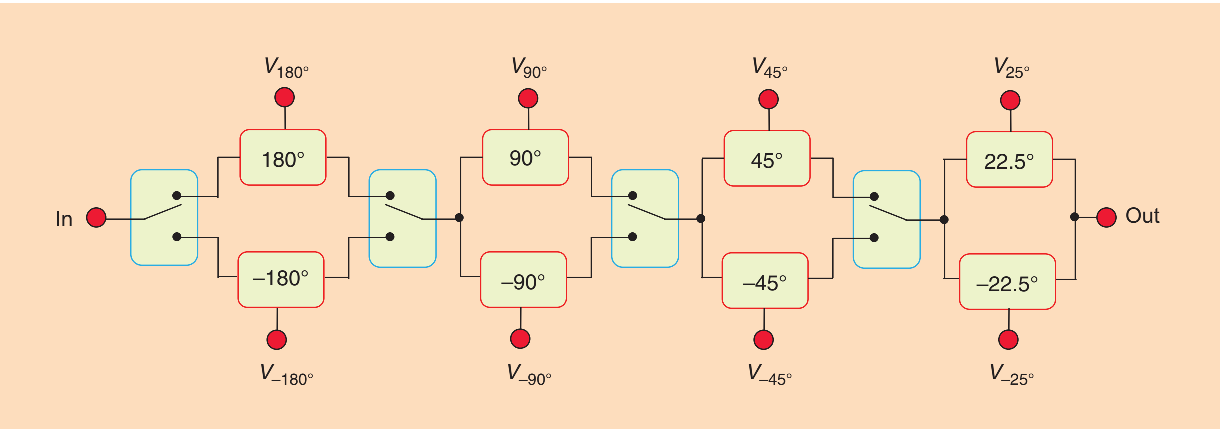

Figure 12. *Digital adjustable phase shifter with 4-bit resolution [2].*

TABLE 2. Comparison of performance of fully integrated phase shifters, TLPS: tuned equivalent transmission line phase shifter based on distributed low-pass sections, RTPS: reflective-type phase shifter VM: vector modulator, *at center/target frequency.

Ref.	Phase Control [°]	Bandwidth [GHz]	Gain ± Ripple* [dB]	Power Supply [mW]	Control Voltages	Chip Area [mm^2]	Technology	Comment
				Vector modulators				
[8]	360	5–6	1.5 n.a.	18	n.a.	1	0.18 μm CMOS	Active
[9]	360	15–20	−6 ± 4	<112	2 analog	0.72	0.18 μm CMOS	Active
[10]	360	50–56	−4.9 ± 0.9	23	n.a. analog	0.4	90 nm CMOS	Active
[11]	360	5.1–5.3	0.6 n.a.	10	3 analog	1.3	0.6 μm GaAs MESFET	Active
[12]	360	4.7–5.7	−9 n.a.	≈ 0	3 analog	1	0.6 μm GaAs MESFET	Passive
[19]	360	4.8–5.8	0 n.a.	9	3 analog	2.4	0.6 μm GaAs MESFET	Active
				Distributed phase shifters				
[21]	360	5–6	−4 ± 1.7	≈ 0	1 analog	0.8	0.6 μm GaAs MESFET	LP sections, passive
[22]	>360	4.2–6.2	−7.3 ± 2	≈ 0	1 analog	1	0.18 μm BiCMOS	LP sections, passive
[23]	>195	5.2–5.8	−3.6 ± 1.5	≈ 0	1 analog	0.6	0.25 μm BiCMOS	LP sections, passive
[24]	96	2.6 ± n.a.	−3.3 ± 0.5	31.5	2 analog	1	0.13 μm CMOS	LP sections with active inductors
[26]	360	8 ± n.a.	n.a.	170	1 analog	0.25	0.18 μm CMOS	LP sections, active, differential
[25]	360 4 bit	11.6–12.6	3.5 ± 0.5	26.6	8 digital	1.8	0.18 μm CMOS	Distributed active switches
[39]	360	3.5–4.5	−0.3 ± 0.8	16–25	n.a.	0.24	0.18 μm CMOS	HP with active inductors
[40]	96	3.875–4.125	−2.8 ± 1.5	>0 n.a.	4 analog	0.3	0.18 μm CMOS	HP with active inductor
				Coupler-based reflective-type phase shifters				
[29]	210	6.1–6.3	−4.9 ± 0.9	≈ 0	1 analog	0.9	0.6 μm GaAs MESFET	Passive
[28]	360	5.15–5.7	−6.4 ± 3	≈ 0	1 analog	0.9	0.6 μm GaAs MESFET	Passive
[30]	>120	14.9–15.7	−5 ± 1	≈ 0	1 analog	0.36	0.25 μm BiCMOS	Passive
				Circulator-based reflective-type phase shifters				
[34]	>90	2.5–10	0 ± 0.5	5.6–8.3	1 analog	0.48	0.18 μm BiCMOS	Active
				Switched-type phase shifters				
[35]	360 5 bit	17–21	−5 ± 0.6	≈ 0	10 digital	1.3	0.25 μm PHEMT	Passive
[36]	360 5 bit	9–15	−14.5 ± 0.5	≈ 0	10 digital	4.3	0.18 μm CMOS	Passive

Phase Control Range/ Frequency Multiplication

One important design parameter for phase shifters is the phase control range. For many applications a phase control range of 360° is required. However, the phase control range has to be traded off with other parameters, which makes the design challenging. Is it possible to multiply the phase control range in a relatively simple way?

Consider that frequency multiplication divides the signal period duration. Consequently, the phase control range is multiplied by the factor of the frequency multiplication. Typically, the method of frequency/ phase multiplication relaxes the contradicting constraints regarding the phase control range and amplitude variations. The drawback is the additional power consumed by the frequency multipliers [38], which should have good linearity and low noise to avoid signal deteriorations.

Hardware Comparison

The measured results of state-of-the-art phase shifter implementations are summarized in Table 2. In this article, we have focused on implementations using standard integrated circuit technologies. Interesting properties can be achieved using microelectromechanical system (MEMS) technology featuring high performance passives. Regarding MEMS technologies and corresponding low loss phase shifter implementations, the reader is referred to [41]–[43].

Conclusions

In this article, the development constraints, architectures, design guidelines, and hardware results of fully integrated phase shifters have been presented. The pros and cons of different approaches have been discussed. To make a long story short:

- Active vector modulators have the capability to provide gain and even gain control, and do not require any varactors. Hence, vector modulators are well suited for a large range of applications and chip technologies.
- Tuned equivalent transmission line phase shifters are typically passive and do not yield gain but have the advantage of a very large bandwidth of several octaves due to the distributed nature.
- Coupler-based reflective type phase shifters do have a simple architecture but tend to have a relatively small bandwidth if the coupler is realized by lumped elements.
- Active circulator-based reflective type phase shifters can be controlled by the transconductance of the amplifiers driving the reflective load thereby enabling a wide bandwidth and relatively low loss.

The optimum choice of the phase shifter architecture depends on the required specifications and the available technologies.

- At the expense of additional dc power and noise, active inductors can be used to increase the phase control range for the tuned equivalent transmission line and reflective type phase shifters.
- Switched-type phase shifters tend to have a relatively large size, especially at low to moderate frequencies but do not require a DAC for phase control from the system point of view.
- For some specific systems including wireless communication front ends, phase/frequency multiplication techniques may be interesting to boost the phase control range while yielding a low-gain ripple.

Finally, the optimum choice of the phase shifter architecture depends on the required specifications and the available technologies.

Acknowledgment

This work was in part funded by the European Community's Seventh Framework Programme under Grant Agreement No. 213952 (MIMAX).

References

[1] S. K. Koul and B. Bhat, *Microwave and Millimeter Wave Phase Shifters*, vol. II. Norwood, MA: Artech House, 1991.

[2] F. Ellinger, *Radio Frequency Integrated Circuits and Technologies*, 2nd ed. Heidelberg, Germany: Springer-Verlag, 2008.

[3] F. Ellinger, U. Jörges, U. Mayer, and R. Eickhoff, "Analysis and compensation of phase variations versus gain in amplifiers verified by SiGe HBT cascode RFIC," *IEEE Trans. Microwave Theory Tech.*, vol. 57, no. 8, pp. 1885–1894, Aug. 2009.

[4] F. Ellinger, C. Carta, L. Rodoni, G. von Büren, D. Barras, M. Schmatz, and H. Jäckel, "BiCMOS variable gain LNA at C-band with ultra low power consumption for WLAN," in *Proc. IEEE Int. Telecommunication Conf.*, Aug. 2004, CD-ROM.

[5] F. Ellinger and H. Jäckel, "Low cost BiCMOS variable Gain LNA at Ku-band with ultra low power consumption for adaptive antenna combining," *IEEE Trans. Microwave Theory Tech.*, vol. 52, no. 2, pp. 702–708, Feb. 2004.

[6] U. Mayer, F. Ellinger, and R. Eickhoff, "Analysis and Reduction of Phase Variations of Variable Gain Amplifiers verified by CMOS Implementation at C-Band," *IET J. Circuits, Devices Syst.*, to be published.

[7] K.-J. Koh and G. M. Rebeiz, "0.13 μm CMOS phase shifters for X-, Ku-, and K-band phased arrays," *IEEE J. Solid-State Circuits*, vol. 42, pp. 2535–2545, Nov. 2007.

[8] N. Joram, U. Mayer, R. Eickhoff, and F. Ellinger, "Fully integrated active CMOS vector modulator for 802.11a compliant diversity transceivers," in *Proc. IEEE Int. Conf. Microwaves, Communications, Antennas and Electronic Systems*, Nov. 2009, pp. 1–4.

[9] P.-S. Wu, H.-Y. Chang, M.-D. Tsai, T.-W. Huang, and H. Wang, "New miniature 15–20-GHz continuous-phase/amplitude control

MMICs using 0.18-μm CMOS technology," *IEEE Trans. Microwave Theory Tech.*, vol. 54, no. 1, pp. 10–19, Jan. 2006.

[10] P. B. Vadivelu, P. Sen, S. Sarkar, D. Dawn, S. Pinel, and J. Laskar, "Integrated CMOS mm-wave phase shifters for single chip portable radar," in *IEEE MTT-S Int. Microwave Symp. Dig.*, June 2009, pp. 565–568.

[11] F. Ellinger, U. Lott, and W. Bächtold, "An antenna diversity MMIC vector modulator for HIPERLAN with low power consumption and calibration capability," *IEEE Trans. Microwave Theory Tech.*, vol. 49, no. 5, pp. 964–969, May 2001.

[12] F. Ellinger, R. Vogt, and W. Bächtold, "A high yield, ultra small, passive, vector modulator based phase shifter for smart antenna combining at C-band," in *Proc. IEEE/CSIRO Asia Pacific Microwave Conf.*, Dec. 2000, pp. 794–797.

[13] F. Ellinger and W. Bächtold, "Novel principle for vector modulator based phase shifter operating with one control voltage," *IEEE J. Solid-State Circuits*, vol. 37, no. 10, pp. 1256–1259, Oct. 2002.

[14] G. Rebeiz and K. J. Koh, "Silicon RFICs for phased arrays," *IEEE Microwave Mag.*, vol. 10, no. 3, pp. 96–103, May 2009.

[15] T. Yu and G. M. Rebeiz, "A 22–24 GHz 4 element CMOS phase array with on-chip coupling characterization," *IEEE J. Solid-State Circuits*, vol. 43, no. 9, pp. 2134–2143, Sept. 2008.

[16] K. J. Koh and G. M. Rebeiz, "An X- and Ku-band 8-element phased-array receiver in 0.18 μm SiGe BiCMOS technology," *IEEE J. Solid-State Circuits*, vol. 43, no. 6, pp. 1360–1371, June 2008.

[17] K. J. Koh, J. W. May and G. M. Rebeiz, "A millimeter-wave (40–45 GHz) 16-element phased-array transmitter in 0.18 μm SiGe BiCMOS technology," *IEEE J. Solid-State Circuits*, vol. 44, no. 5, pp. 1498–1509, May 2009.

[18] F. Ellinger and W. Bächtold, "Adaptive antenna receiver module for WLAN at C-Band with low power consumption," *IEEE Microwave Wireless Compon. Lett.*, vol. 12, no. 9, pp. 348–350, Sept. 2002.

[19] F. Ellinger, R. Vogt, and W. Bächtold, "Calibratable adaptive antenna combiner at 5.2 GHz with high yield for laptop interface card," *IEEE Trans. Microwave Theory Tech.* (Special Issue), vol. 48, no. 12, pp. 2714–2720, Dec. 2000.

[20] A. S. Nagra and R. A. York, "Distributed analog phase shifters with low insertion loss," *IEEE Trans. Microwave Theory Tech.*, vol. 47, no. 9, pp. 1705–1711, Sept. 1999.

[21] F. Ellinger, H. Jäckel, and W. Bächtold, "Varactor loaded transmission line phase shifter at C-band using lumped elements," *IEEE Trans. Microwave Theory Tech.*, vol. 51, no. 4, pp. 1135–1140, Apr. 2003.

[22] J. Wagner, U. Mayer, and F. Ellinger, "Passive transmission line phase shifter at C-band in CMOS using lumped elements," in *Proc. 17th Int. Conf. IEEE Microwaves, Radar and Wireless Communications*, May 2008, pp. 1–4.

[23] F. Ellinger, J. Wagner, U. Mayer, and R. Eickhoff, "Passive varactor tuned equivalent transmission line phase shifter at C-band in 0.25 μm BiCMOS," *IET J. Circuits, Devices Syst.*, vol. 2, no. 4, pp. 355–360, 2008.

[24] M. A. Y. Abdalla, K. Phang, and G. V. Eleftheriades, "Printed and integrated CMOS positive/negative refractive-index phase shifters using tunable active inductors," *IEEE Trans. Microwave Theory Tech.*, vol. 55, no. 8, pp. 1611–1623, Aug. 2007.

[25] D.-W. Kang and S. Hong, "A 4-bit CMOS phase shifter using distributed active switches," *IEEE Trans. Microwave Theory Tech.*, vol. 55, no. 7, pp. 1476–1483, July 2007.

[26] S. Hamedi-Hagh and C. A. T. Salama, "A novel C-band CMOS phase shifter for communication systems," in *Proc. Int. Symp. Circuits and Systems*, May 2003, vol. 2, pp. II-316–II-319.

[27] C. Lu and A.-V. H. Pham, "Development of multiband phase shifters in 180 nm RF CMOS technology with active loss compensation," *IEEE Trans. Microwave Theory Tech.*, vol. 54, no. 1, pp. 40–45, Jan. 2006.

[28] F. Ellinger, R. Vogt, and W. Bächtold, "Ultra compact reflective type phase shifter MMIC at C-band with 360° phase control range for smart antenna combining," *IEEE J. Solid-State Circuits*, vol. 37, no. 4, pp. 481–486, Apr. 2002.

[29] F. Ellinger, R. Vogt, and W. Bächtold, "Compact reflective type phase shifter MMIC for C-band using a lumped element coupler," *IEEE Trans. Microwave Theory Tech.*, vol. 49, no. 5, pp. 913–917, May 2001.

[30] F. Ellinger, "A 15 GHz reflective type phase shifter MMIC fabricated on 0.25 μm SiGe BiCMOS technology," in *Proc. Int. Conf. Telecommunication*, May 2005, CD-ROM.

[31] H. Hayashi, M. Muraguchi, Y. Umeda, and T. Enoki, "A high-Q broad-band active inductor and its application to a low-loss analog phase shifter," *IEEE Trans. Microwave Theory Tech.*, vol. 44, no. 12, pp. 2369–2374, Dec. 1996.

[32] S. Tanaka, N. Shimomura, and K. Ohtake, "Active circulators-the realization of circulators using transistors," *Proc. IEEE*, vol. 53, no. 3, pp. 260–267, Mar. 1965.

[33] Y. Zeng and C. E. Saavedra, "An ultra-compact CMOS variable phase shifter for 2-4-GHz ISM applications," *IEEE Trans. Microwave Theory Tech.*, vol. 56, no. 6, pp. 1349–1354, June 2008.

[34] U. Mayer, F. Ellinger, and R. Eickhoff, "Compact circulator based phase shifter at C-band in BiCMOS," in *Proc. IEEE Radio Frequency Integrated Circuits Symp.*, June 2009, pp. 499–502.

[35] C. F. Campell and S. A. Brown, "A compact 5-bit phase-shifter MMIC for K-band satellite communication systems," *IEEE Trans. Microwave Theory Tech.*, vol. 48, no. 12, pp. 2652–2656, Dec. 2000.

[36] D.-W. Kang, H. D. Lee, C.-H. Kim, and S. Hong, "Ku-band MMIC phase shifter using a parallel resonator with 0.18-μm CMOS technology," *IEEE Trans. Microwave Theory Tech.*, vol. 54, no. 1, pp. 294–301, Jan. 2006.

[37] D.-W. Kang, J.-G. Kim, B.-W. Min, and G. M. Rebeiz, "Single and four-element Ka-band transmit/receive phased-array silicon RFICs with 5-bit amplitude and phase control," *IEEE Trans. Microwave Theory Tech.*, vol. 57, no. 12, pp. 3534–3543, Dec. 2009.

[38] F. Ellinger and W. Bächtold, "Compact and low power consuming frequency/phase multiplier MMICs for wireless LAN at S-band and C-band," *IEE Proc. Devices, Circuits Syst.*, vol. 150, no. 3, pp. 199–204, June 2003.

[39] L.-H. Lu and Y.-T. Liao, "A 4-GHz phase shifter MMIC in 0.18-μm CMOS," *IEEE Microwave Wireless Compon. Lett.*, vol. 15, no. 10, pp. 694–696, Oct. 2005.

[40] M. Abdalla, K. Phang, and G.-V. Eleftheriades, "A bi-directional electronically tunable CMOS phase shifter using the high-pass topology," in *IEEE MTT-S Int. Microwave Symp. Dig.*, June 2007, pp. 2173–2176.

[41] G. Rebeiz, K. Entesari, I. Reines, S.-J. Park, M. El-tanani, A. Grichener, and A. Brown, "Tuning in to RF MEMS," *IEEE Microwave Mag.*, vol. 10, no. 6, pp. 55–72, Oct. 2009.

[42] N. S. Barker and G. M. Rebeiz, "Optimization of distributed MEMS transmission-line phase shifters-U-band and W-band designs," *IEEE Trans. Microwave Theory Tech.*, vol. 48, pp. 1957–1966, Nov. 2000.

[43] K. Topalli, O. A. Civi, S. Demir, S. Koc, and T. Akin, "A monolithic phased array using 3-bit distributed RF MEMS phase shifters," *IEEE Trans. Microwave Theory Tech.*, vol. 56, no. 2, pp. 270–277, Feb. 2008.